Dense Estimation of Surface Reflectance Properties for Merging Virtualized Objects into Real Images

Takashi Machida†, Haruo Takemura‡ and Naokazu Yokoya†
†Graduate School of Information Science, Nara Institute of Science and Technology
E-mail: {taka-ma, yokoya}@is.aist-nara.ac.jp
‡Cybermedia Center, Osaka University
E-mail: takemura@cmc.osaka-u.ac.jp

Abstract

To appropriately reproduce a real object in a mixed environment, it is necessary to estimate reflectance properties of object surfaces. This paper describes a new method of densely estimating non-uniform surface reflectance properties of an object with convex and concave surfaces using registered range and surface color texture images obtained by a laser rangefinder. The proposed method determines positions of light source to take color images for discriminating diffuse and specular reflection components of surface reflection. The Torrance-Sparrow model is employed to estimate reflectance parameters using color images under multiple illumination conditions. Experiments show the usefulness of the method.

1 Introduction

In mixed reality (MR), it is needed that a virtualized object is merged in real world without a feeling of wrongness [1]. To represent a virtualized object photo-realistically, there are two approaches. One is called an image based rendering (IBR) that has often been used to reproduce real objects in computer graphics (CG). Generally, IBR methods require a large number of real images to represent the virtualized object under arbitrary illumination conditions and arbitrary viewing directions. Mukaigawa et al. [10] have proposed a photometric IBR in which a virtualized object is represented with a few real images. However, in the case of using a limited number of images, a problem occurs; i.e., the appearance of object is not faithfully reproduced since some part of the object is interpolated linearly. The other method is called a polygon based rendering (PBR). This method reproduces the object shape and surface reflectance properties. If the object surface reflectance properties are estimated at once, the virtualized object can be rendered appropriately under virtualized illumination conditions estimated from real environments [11, 3]. A number of methods of estimating reflectance properties of an object surface have been developed [2, 5, 6, 7, 8, 9, 12]. In these methods, surface reflectance models with several parameters are employed and shape and color information of the object is used to estimate the reflectance parameters.

In some works [2, 5, 9], it is assumed that an object has a uniform reflectance property over the entire surface. Reflectance parameters are estimated by using the standard least-squares method to fit a reflectance model to a given color image. Due to the assumption, such methods cannot be applied to objects which consist of several different materials and have non-uniform reflectance properties. To treat non-uniform surface objects, Kay and Caelli [6] have proposed a method which uses multiple images of an object under different lighting conditions and estimates reflectance parameters by solving simultaneous equations. However, the method still has a problem that results are not stable especially when the specular reflection component, which is one of the reflection components, is very small.

Recently, Sato et al. [12] have developed a methodology to estimate non-uniform reflectance properties. They set up an object on a robot arm and measure the object with a CCD camera and a rangefinder from a large number of viewpoints by rotating the robot arm. In the method, reflectance parameters are stably acquired by decomposing the surface reflection into two components based on the singular value decomposition (SVD) technique. Although the method can be applied to objects with non-uniform reflectance properties, the shape of object should be limited. This is because it is difficult to observe the specular reflection component over the entire surface, since the lighting condition for a pose of the object against the camera cannot be changed in the method.

We propose a new method for estimating non-uniform reflectance properties by observing the specular reflection component densely in the image obtained by a laser

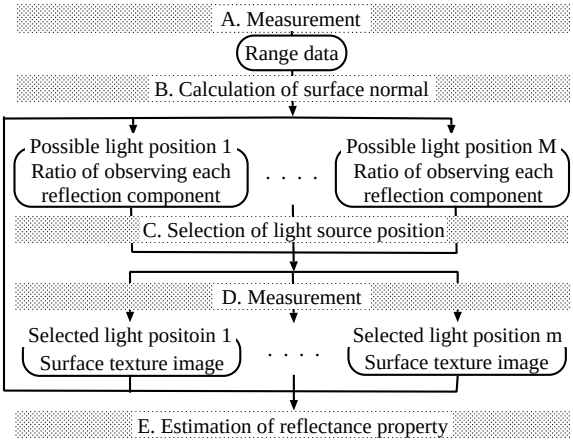

Figure 1. Flow diagram of estimating surface reflectance properties.

rangefinder which accurately takes registered range and color images of an object. In this paper, an algorithm is proposed to determine light positions with which the specular reflection component is strongly observed over the surface of a complex object with convex and concave surfaces.

2 Estimation of reflectance parameters from range and color images

In the present work, the Torrance-Sparrow model is employed as a surface reflectance model to estimate object surface reflectance properties from range and color images. Figure 1 shows a flow diagram of estimating surface reflectance properties. Our process consists of four parts, which are a measurement of an object (A, D), a preprocessing (B), a selection of light source (C), and an estimation of reflectance parameters (E).

2.1 Torrance-Sparrow model

In this paper, the Torrance-Sparrow model [13], which physically represents object reflectance properties, is employed to estimate reflectance parameters. The Torrance-Sparrow model is given as:

$$i = \frac{Y}{C^2}\{P_d \cos\theta_d + \frac{P_s}{\cos\theta_v} exp(-\frac{\theta_r^2}{2\sigma^2})\}, \quad (1)$$

where i represents an observed intensity, C is an attenuation coefficient concerning the distance between a point light source and an object surface point, Y represents the strength of a light souce. P_d is the diffuse reflectance parameter, P_s is the specular reflectance parameter, σ is the surface roughness parameter which is the standard deviation of a Gaussian distribution, θ_d is an angle between a light source vector $\mathbf{L}$ and a surface normal vector $\mathbf{N}$, θ_v is

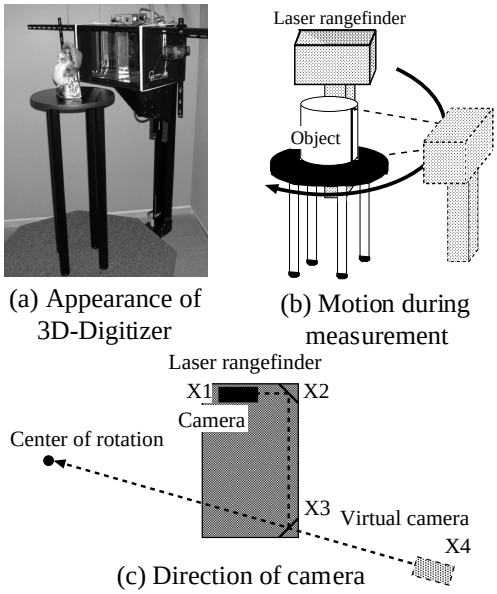

Figure 2. 3D-Digitizer.

an angle between a viewing vector $\mathbf{V}$ and a surface normal vector $\mathbf{N}$, and θ_r is an angle between a viewing vector $\mathbf{V}$ and a reflection vector $\mathbf{L}'$, where the reflection vector is the vector which $\mathbf{L}$ is mirrored against $\mathbf{N}$. All vectors are normalized as unit vectors.

2.2 Measurement of an object

We use a laser rangefinder (Cyberware 3030RGB) with known positions of point light sources and a camera for acquiring surface color images, as illustrated in Figure 2(a). Figure 2(b) shows its motion during measurement. This system can obtain registered range and surface color texture images at the same time by rotating the rangefinder and the camera around an object, so that there is no registration error, even when an object is measured many times. Figure 2(c) shows the illustration viewed from the top of the device. A camera is located at $X1$ and a texture image is acquired through mirrors which are located at $X2$ and $X3$. We assume that the camera is located at $X4$ virtually and the camera looks toward the center of rotation.

2.3 Preprocessing

Generally, the noise and quantization error are included in the range image acquired from the laser rangefinder. There is also a problem that the surface normal is not calculated accurately around the discontinuity in the range image. Therefore, we employ an adaptive local quadratic surface fitting.

Firstly, the 5×5 median filter is applied to the range image to remove the noise. Secondly, the quadratic surface is

locally fitted with the range image. The range image from the Cyberware rangefinder is expressed by the cylindrical coordinates. Each point of the range image is represented as:

$$(x, y, z) = \{-r(s,t)\sin(s), -t, -r(s,t)\cos(s)\}, \quad (2)$$

where r, s, t are the distance from the center of rotation, the angle of rotation, and the height along the rotation axis, respectively.

The unit normal vector is given as follows:

$$\mathbf{N} = \frac{1}{\sqrt{r_s^2 + r^2 + r^2 r_t^2}}\{-r_s\sin(s) - r\cos(s), \; -r_t r, \; -r_s\cos(s) + r\sin(s)\}, \quad (3)$$

where r_s, r_t are gradient components of the range image $r(s,t)$. This gradient is computed using the following local surface fit:

$$r'(s,t) = as^2 + bt^2 + cst + ds + et + f, \quad (4)$$

Coefficients $a \sim f$ are determined by minimizing the following equation using the range data $r(s,t)$ and Equation (4).

$$error(s,t) = \sum_{u=-2}^{2}\sum_{v=-2}^{2}\{r(s+u, t+v) - r'(s+u, t+v)\}^2, \quad (5)$$

where u, v are local coordinates in a 5×5 window. In our approach, selected local quadratic surface fit is achieved by using the Yokoya-Levine operator [14]. In [14], the best window is selected among 25 possible windows which include the point (s,t) to estimate the coefficients $a \sim f$ at (s,t). The best window provides the minimum fitting error in Equation (5).

2.4 Selection of light source

To densely estimate non-uniform reflectance parameters independently, it is required to observe each pixel under three different lighting conditions: One for observing only the diffuse reflection component to determine one unknown parameter P_d and others for observing both the diffuse and specular reflection components to acquire two unknown parameters P_s and σ. Therefore, in the present experimental setup, multiple positions of a light are determined among 60 possible positions prepared around the laser rangefinder and these are arranged with 5 vertically and with 12 horizontally at the interval of 5 cm as shown in Figure 3. The position of a camera is calibrated in advance by measuring a box whose size is known. The position of a light souce

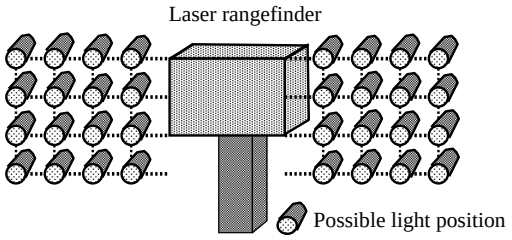

Figure 3. Multiple possible light source positions.

is calibrated based on the distance from the center of rotation in world coordinates. When optimum light positions are selected, a single light is attached at selected possible positions in turn. Therefore, the calibration of brightness among multiple lights is not needed.

Let I_p be a color image which is to be obtained with a possible light position p $(p = 1, \cdots, 60)$ and consists of n pixels $(i_{p1}, \cdots, i_{pn})$, where i_{pk} means a color intensity, D_p be the number of pixels which include only the diffuse reflection component in I_p, and S_p be the number of pixels which include the specular reflection component strongly in I_p.

First, the following conditions are examined for each pixel in the object surface texture under each light position p.

- **Measurability of light reflection**
- **Measurability of only diffuse reflection**
- **Measurability of strong specular reflection**

Second, the light positions p and q which satisfy $D_p = Max(D_1, \cdots, D_{60})$ and $S_q = Max(S_1, \cdots, S_{60})$ are selected. In the next light source position selection, the position which satisfies the same condition is selected among the rest except for light source positions decided so far. Then, m light positions are selected to densely estimate reflectance parameters. The selections of positions are repeated until almost all pixels are observed once for only the diffuse reflection component and twice for the strong specular reflection component.

We introduce a threshold th, i.e., the ratio of the measurability of both reflection components to stop the process of selecting light positions. With respect to determining the threshold th, we judge the ratio of the measurability of the specular reflection with all possible positions. This ratio is a limit of measuring the specular reflection component. Using the threshold, we can terminate the light selection process in the case that the ratio of measurability of specular reflection component cannot increase more, even if the number of positions of light source is increased. In such a way, reflectance parameters can be efficiently estimated almost the whole object surface using a limited number of texture images.

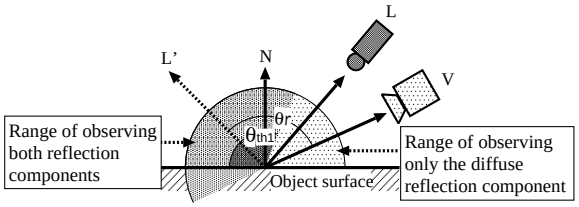

Figure 4. Observation of only the diffuse reflection component.

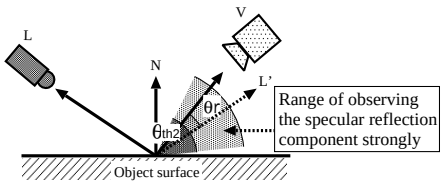

Figure 5. Observation of the specular reflection component strongly.

2.4.1 Measurability of light reflection

In order to measure the light reflection at a specific point of the object surface, the point on the surface must be observable from the camera position. Additionally positional relationship among the camera, the point and the light source must satisfy the following conditions.

$$(\mathbf{V}_k \cdot \mathbf{N}_k) > \mathbf{0},\ (\mathbf{L}_{pk} \cdot \mathbf{N}_k) > \mathbf{0}, \tag{6}$$

where $\mathbf{V}_k$, $\mathbf{L}_{pk}$, and $\mathbf{N}_k$ are the viewing direction, the light source direction, and the surface normal at the k-th pixel, respectively. Note that the viewing direction $\mathbf{V}_k$ and the surface normal $\mathbf{N}_k$ are independent of the light source position p. Even when the above equations are both satisfied, there is a possibility that a shadow is casted on the pixel. In other words, a point on the object may be covered by a shadow casted by light source p. This can be judged by an existing technique[4].

2.4.2 Measurability of diffuse reflection only

When the k-th pixel consists of only the diffuse reflection, the reflection vector $\mathbf{L'}_{pk}$ satisfies the following equation.

$$\theta_r = cos^{-1}(\mathbf{V}_k \cdot \mathbf{L}'_{pk}) > \theta_{th1}, \tag{7}$$

where θ_{th1} is a threshold angle between $\mathbf{V}_k$ and $\mathbf{L}'_{pk}$. Equation (7) implies that only the diffuse reflection component is observed if θ_r is greater than θ_{th1} as illustrated in Figure 4. When this condition stands and the pixel is not in a shadow, the pixel is judged to have diffuse reflection only and is counted in D_p.

2.4.3 Measurability of strong specular reflection

When k-th pixel includes the specular reflection strongly, the reflection vector $\mathbf{L'}_{pk}$ satisfies the following equation.

$$\theta_r = cos^{-1}(\mathbf{V}_k \cdot \mathbf{L}'_{pk}) \leq \theta_{th2}, \tag{8}$$

where θ_{th2} is a threshold angle between $\mathbf{V}_k$ and $\mathbf{L}'_{pk}$. Equation (8) means that both the diffuse and specular reflection components are observed if θ_r is smaller than θ_{th2} as illustrated in Figure 5. The above condition is based on the fact that the specular reflection is observed strongly in a limited range of a viewing angle. When this condition stands and the pixel is not in a shadow, the pixel is judged to have strong specular reflection and is counted in S_p.

2.5 Estimation of reflectance parameters

Let $I_{p,diff}$ be the set of pixels which are judged to consist of only the diffuse reflection component with the light position p and consist of α pixels $(i_{p,diff,1}, \cdots, i_{p,diff,\alpha})$, where $i_{p,diff,k}$ means a color intensity. Let $I_{p,both}$ be the set of pixels which are judged to include the specular reflection component strongly and consist of β pixels $(i_{p,both,1}, \cdots, i_{p,both,\beta})$, where $i_{p,both,k}$ means a color intensity. Note that there are some pixels which consist of neither the diffuse reflection component only, nor the strong specular reflection component in $I_{p,diff}$ and $I_{p,both}$. With respect to such a pixel, reflectance parameters cannot be estimated.

The diffuse reflectance parameter P_{dk} at the k-th pixel is estimated from the value of $i_{p,diff,k}$ in the image $I_{p,diff}$, $\mathbf{N}_k$ and $\mathbf{L}_{pk}$. In order to get the most reliable estimation, the pixel whose angle θ_r is the smallest but greater than θ_{th1} is selected.

The specular reflectance parameter P_{sk} and the surface roughness parameter σ_k at the k-th pixel are estimated by solving a simultaneous equation of Equation (1) with the value of the specular reflection component extracted from the k-th pixels $i_{p,both,k}$ and $i_{q,both,k}$ in the images $I_{p,both}$ and $I_{q,both}$, $\mathbf{N}_k$, $\mathbf{L}_{pk}$, $\mathbf{V}_k$, and P_{dk} estimated above. In order to get the most reliable estimation, the pixels whose angle θ_r is the smallest or the second smallest and is smaller than θ_{th2}, are selected.

3 Experiments

In our experiments, a measured object is a plastic doll and exibits non-uniform surface reflectance as shown in Figure 6(a) and is assumed not to have interreflections. We fix some parameters as $\theta_{th1} = 60^o$, $\theta_{th2} = 20^o$, $th = 80\%$. The proposed method of selecting positions of the light source determined 12 light source positions for the object.

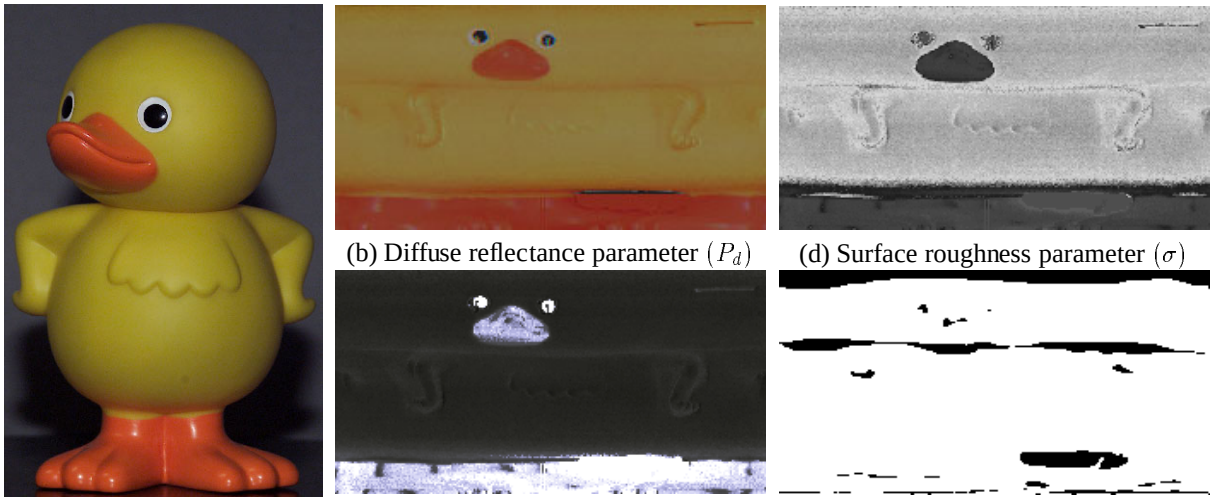

(a) Object (b) Diffuse reflectance parameter (P_d) (c) Specular reflectance parameter (P_s) (d) Surface roughness parameter (σ) (e) Area of observing specular reflection

Figure 6. A measured object and estimated reflectance parameters.

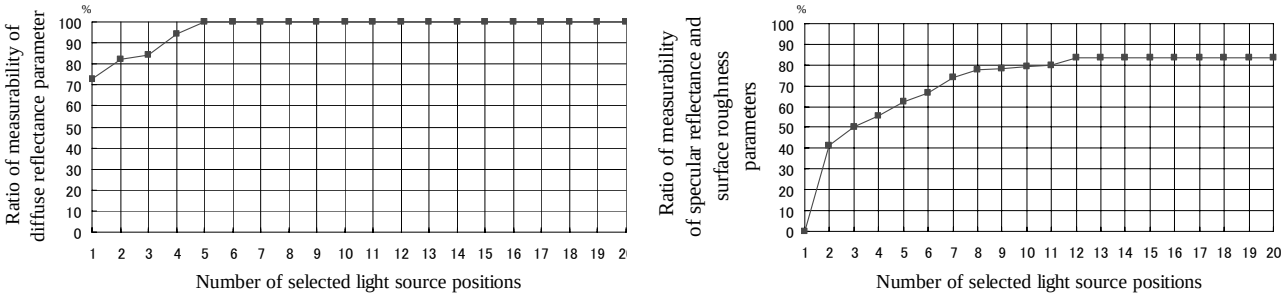

(a) Possibility of estimating the diffuse reflectance parameter

(b) Possibility of estimating the specular reflectance and the surface roughness parameter

Figure 7. The possibility of estimating each reflectance parameter with respect to the number of light positions.

Figure 6(b) illustrates the diffuse reflectance parameter estimated all over the object surface. Figure 6(c) is the specular reflectance parameter. This image clearly shows that the specular reflectance parameter of the doll's beak and leg are different from the rest. Actually, the beak and legs are highly reflective as in Figure 6(a). Figure 6(d) shows the surface roughness parameter with gray-scale where the largest value is coded as white. This image means that the smaller the value is, the smoother the object surface is. Figure 6(e) shows the ratio of pixels where specular reflectance and surface roughness parameters are computed. The black part means that both parameters are not directly estimated. Non-uniform specular reflectance and surface roughness parameters were estimated without interpolation for 83.46% of the surface. Note that there is a part where reflectance parameters cannot be estimated. These parts are linearly interpolated.

Figure 7 illustrates the measurability of both reflection components with respect to the number of light sources. Note that the horizontal axis is represented until 20, since these graphs are stable even if all possible positions are used. In Figure 7(a), with respect to the diffuse reflectance parameter, when the number of selected light source positions is 5, the ratio of the measurability of the diffuse reflection component is 100%. In Figure 7(b), as for the specular reflectance and the surface roughness parameters, even when the object is measured with all possible positions, the ratio of the measurability of the specular reflection component is 83.53%. In our method, the ratio of measurability of the specular reflection component is 83.46% with automatically selected 12 light source positions. Since this figure is comparable to that with all possible light source positions, the experiment shows that the proposed method is efficient.

Figure 8(b) and (c) show results of merging the virtual-

(a) geodesic dome (b) result 1 (c) result 2

Figure 8. Merging a virtualized object into a real image.

ized object into a real image. The real illumination condition is modeled by light sources on a geodesic dome surrounding the object as shown in Figure 8(a). Virtual light sources are uniformly spaced on the geodesic dome and these brightness are the same. The number of virtual lights is 42. Because surface reflectance parameters are estimated densely, the virtualized object is represented without a feeling of wrongness. Frame rate is 3.2 fps on a Pentium III 1GHz PC. Therefore, if an efficient rendering method is achieved, the virtualized object can be merged into real world in real time.

4 Conclusions

In this paper, we have proposed a new method of densely estimating non-uniform reflectance properties for almost the whole object surface by using the laser rangefinder for virtualizing real objects. In our approach, multiple light source positions around the laser rangefinder are automatically selected, so that diffuse and specular reflection components are observed densely. The experiments have shown that the proposed method is useful for estimating the reflectance parameters of objects which exhibit non-uniform surface reflectance. In the future, we will investigate a method to consider interreflections all over the object surface. Moreover, we have to automatically estimate real illumination conditions for merging virtualized objects into real images for mixed reality applications.

Acknowledgments: This work was supported in part by the Grant-in-Aid for Scientific Research under the contract no.13480098 from the ministry of Education, Science, Sports and Culture.

References

[1] R. T. Azuma. A survey of augmented reality. *Presence*, 6(4):355–385, 1997.

[2] R. Baribeau, M. Rioux, and G. Godin. Color reflectance modeling using a polychromatic laser sensor. *IEEE Trans. on Pattern Anal. Mach. Intell.*, 14(2):263–269, 1992.

[3] P. Debevec. Rendering synthetic objects into real scenes: Bridging traditional and image-based graphics with global illumination and high dynamic range photography. *Proc. SIGGRAPH '98*, pages 189–198, 1998.

[4] J. Foley, A. van Dam, S. Feiner, and J. Hughes. *Computer Graphics Principles and Practice*. Addison-Wesley Publishing Company, 2nd edition, 1993.

[5] K. Ikeuchi and K. Sato. Determining reflectance properties of an object using range and brightness images. *IEEE Trans. on Pattern Anal. Mach. Intell.*, 13(11):1139–1153, 1991.

[6] G. Kay and T. Caelli. Inverting an illumination model from range and intensity maps. *CVGIP: Image Understanding*, 59:183–201, 1994.

[7] S. Lin and S. W. Lee. Estimation of diffuse and specular appearance. *Proc. Int. Conf. on Computer Vision*, 2:855–860, 1999.

[8] S. Lin and S. W. Lee. A representation of specular appearance. *Proc. Int. Conf. on Computer Vision*, 2:849–854, 1999.

[9] J. Lu and J. Little. Reflectance function estimation and shape recovery from image sequence of a rotating object. *Proc. Int. Conf. on Computer Vision*, pages 80–86, June 1995.

[10] Y. Mukaigawa, H. Miyaki, S. Mihashi, and T. Shakunaga. Photometric image-based rendering for image generation in arbitrary illumination. *Proc. Int. Conf. on Computer Vision*, pages 643–649, July 2001.

[11] I. Sato, Y. Sato, and K. Ikeuchi. Acquiring a radiance distribution to superimpose virtual objects onto a real scene. *IEEE Trans. on Visualization and Computer Graphics*, 5(1):1–12, January 1999.

[12] Y. Sato, M. D. Wheeler, and K. Ikeuchi. Object shape and reflectance modeling from observation. *Proc. SIGGRAPH '97*, pages 379–387, 1997.

[13] K. E. Torrance and E. M. Sparrow. Theory for off-specular reflection from roughened surfaces. *Journal of Optical Society of America*, pages 1105–1114, 1967.

[14] N. Yokoya and M. D. Levine. Range image segmentation based on differential geometry: A hybrid approach. *IEEE Trans. Pattern Anal. Mach. Intell.*, 11(6):643–649, June 1989.